# MIXING DISPLACEMENT OF VISCOPLASTIC FLUIDS FROM A CHANNEL WITH A RECTANGULAR CAVITY

G. I. Burdé, E. P. Il'yasov,
I. B. Simanovskii, and Yu. I. Terent'ev

UDC 532.556.2

Different mixing displacement regimes for viscoplastic fluids are investigated theoretically and experimentally.

The problem of displacing viscoplastic fluids is of interest in connection with the problem of improving the cementing of oil wells. Here, a very important problem is the problem of the effect of cavities in the well walls on the cementing process.

Mixing displacement is usually examined (see, e.g., [1]) only for channels with constant cross section with a plane-parallel velocity profile (in this case, other simplifying assumptions, such as uniformity in the properties of the liquids, absence of transverse transport of matter, etc., are made as well).

In the present work, the problem of mixing displacement of fluids from a channel with a cavity is solved without any simplifying assumptions involving the structure of the flow or the nature of the transport of matter. The rheological properties of the viscoplastic fluid are approximated by Williamson's model [2]; the displaced and displacing fluids have the same density and viscosity. The results of the calculations are compared with the experimental data obtained by the authors.

1. Let us assume that initially a channel with a rectangular cavity is filled with a fluid moving in a steady-state flow (displaced fluid). The boundaries AH and BCDEFG (Fig. 1a) are solid, the segment AB represents the inlet section of the region, and GH is the outlet, and in the inlet and outlet regions the motion is assumed to be plane-parallel.

The position of the boundaries AB and GH, with which the motion in these sections can be viewed as plane-parallel, was determined by a numerical experiment. Analysis of the results shows that the motion near sections AB and GH becomes, to a good approximation, plane-parallel with lengths BC and FG exceeding L/2. In the calculations, the results of which are presented in the article, it was assumed that BC = FG = L.

The velocity field of the stationary flow was determined from the equations (incompressible fluid)

$$v_k \frac{\partial v_i}{\partial x_k} = -\frac{1}{\rho}\frac{\partial p}{\partial x_i} + \frac{1}{\rho}\frac{\partial \tau_{ik}}{\partial x_k}, \quad \frac{\partial v_k}{\partial x_k} = 0. \tag{1}$$

In order to model the viscoplastic fluid, we chose Williamson's fluid [2]

$$\tau_{ik} = 2\eta e_{ik}, \quad \eta = \eta_\infty + \frac{\tau_0}{W + |2e_{ik}e_{ik}|^{1/2}}, \qquad e_{ik} = \frac{1}{2}\left(\frac{\partial v_i}{\partial x_k} + \frac{\partial v_k}{\partial x_i}\right), \tag{2}$$

which for $W \to 0$ has properties that are nearly the same as Bingham's fluid. (The calculations were performed precisely in this range of variation of parameters.) Writing Eqs. (1) and (2) for a plane flow in terms of the stream function $\psi$, the vorticity $\varphi$, and the dimensionless viscosity $\nu$:

$$v_x = \frac{\partial \psi}{\partial y}, \quad v_y = -\frac{\partial \psi}{\partial x}, \quad \varphi = \frac{\partial v_y}{\partial x} - \frac{\partial v_x}{\partial y}, \quad \nu = \frac{\eta}{\eta_\infty} \tag{3}$$

and transforming to dimensionless variables, we obtain

State Pedagogical Institute, Perm. Translated from Inzhenerno-Fizicheskii Zhurnal, Vol. 40, No. 3, pp. 432-439, March, 1981. Original article submitted February 27, 1980.



0022-0841/81/4003-0264 $07.50 

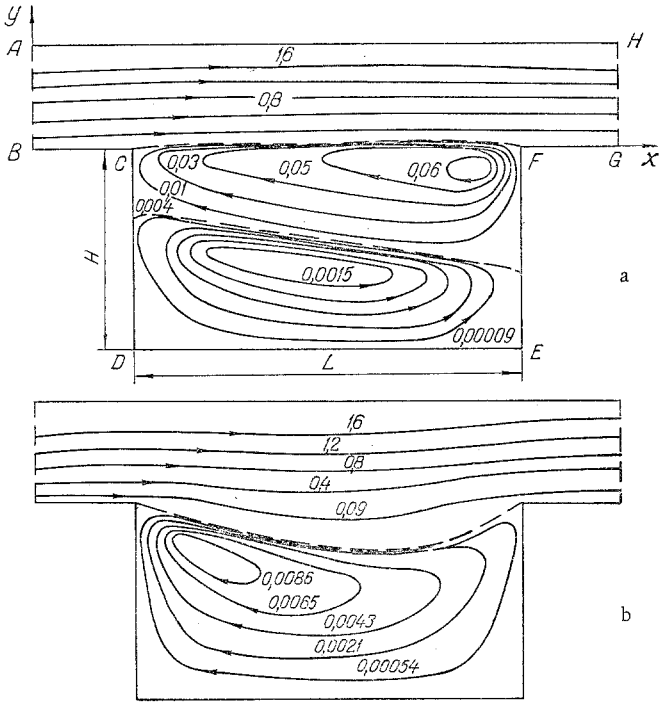


Fig. 1. Flow lines with T = 12: a) Re = 1800; b) Re = 10.

$$\mathrm{Re}\left(\frac{\partial\psi}{\partial x}\frac{\partial\varphi}{\partial y}-\frac{\partial\psi}{\partial y}\frac{\partial\varphi}{\partial x}\right)+\frac{\partial^2(\nu\varphi)}{\partial x^2}+\frac{\partial^2(\nu\varphi)}{\partial y^2}-$$
$$-\varphi\left(\frac{\partial^2\nu}{\partial x^2}+\frac{\partial^2\nu}{\partial y^2}\right)=4\frac{\partial^2\nu}{\partial x\partial y}\frac{\partial^2\psi}{\partial x\partial y}+ \tag{4}$$
$$+\left(\frac{\partial^2\nu}{\partial x^2}-\frac{\partial^2\nu}{\partial y^2}\right)\left(\frac{\partial^2\psi}{\partial x^2}-\frac{\partial^2\psi}{\partial y^2}\right),$$

$$\frac{\partial^2\psi}{\partial x^2}+\frac{\partial^2\psi}{\partial y^2}=-\varphi, \tag{5}$$

$$\nu=1+\frac{T}{\mathrm{B}+\mathrm{Re}\left[4\left(\frac{\partial^2\psi}{\partial x\partial y}\right)^2+\left(\frac{\partial^2\psi}{\partial x^2}-\frac{\partial^2\psi}{\partial y^2}\right)\right]^{1/2}}. \tag{6}$$

Here, the units of length and velocity are chosen as the half-width of the channel h and the average pumping velocity u, determined from the flow rate. Three similarity criteria emerge from Eqs. (4)-(6): $\mathrm{Re} = uh/(\eta_\infty\rho)$, Reynolds number; $\mathrm{T} = \tau_0 h^2\rho/\eta_\infty^2$, the analog of Hedstrem's number for Bingham's fluid; $\mathrm{B} = \mathrm{W}h^2\rho/\eta_\infty$, a parameter in Williamson's model. In the calculations, the quantity B was chosen so that the fluid would have properties nearly the same as Bingham's fluid. The results presented below were obtained for B = T/100. The calculations show that for such a ratio of B and T the plane-parallel velocity profile at the inlet coincides with quite good accuracy with the Bingham profile, and further decrease in B has almost no effect on the flow structure in the channel and the cavity.

Let us examine the boundary conditions for Eqs. (4)-(6).

The stream function and vorticity, corresponding to the solution of Eqs. (1) for a plane-parallel flow, are given at the inlet AB and outlet GH:

$$\psi=\psi_0(y),\quad \varphi=\varphi_0(y), \tag{7}$$

where

$$\psi_0(y)=\frac{r}{4}\left\{\frac{2-3(1-y)+(1-y)^3}{3}-y^2\frac{T+\mathrm{B}}{r\,\mathrm{Re}}+\frac{ac}{(r\,\mathrm{Re})^2}y+\right. \tag{8}$$
$$\left.+\frac{b}{(r\,\mathrm{Re})^3}\left(c-\sqrt{[a-(r\,\mathrm{Re})\,y]^2 b}\right)-\frac{1}{3(r\,\mathrm{Re})^3}\times\right.$$

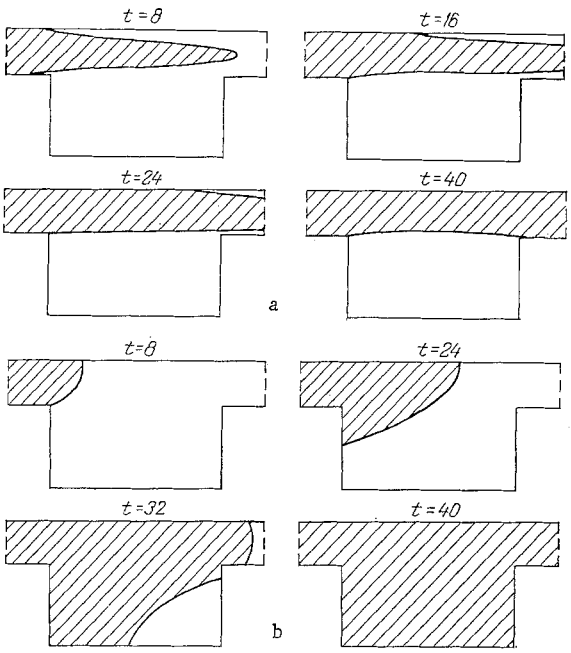


Fig. 2. Development of the displacement process with time: a) for T = 12, Re = 1800; b) for T = 12, Re = 10 (in the shaded part of the channel C > 0.65).

$$\times [c^3 - (\sqrt{[a-(r\,\mathrm{Re})\,y]^2 + b})^3] + \frac{b\,[a-(r\,\mathrm{Re})\,y]}{(r\,\mathrm{Re})^3} \ln\left[\frac{a-(r\,\mathrm{Re})\,y + \sqrt{[a-(r\,\mathrm{Re})\,y]^2 + b}}{a+c}\right]\Bigg\};$$

$$\varphi_0(y) = -\frac{r}{2}\left\{1 - y - \frac{T+\mathrm{B}}{r\,\mathrm{Re}} + \frac{1}{r\,\mathrm{Re}}\sqrt{[a-(r\,\mathrm{Re})\,y]^2 + b}\right\}. \tag{9}$$

The constant quantities $a$, b, c, and r, entering into Eqs. (8), and (9), are determined as follows:

$$a = r\,\mathrm{Re} + \mathrm{B} - T,\ b = 4\mathrm{B}T,\ c = \sqrt{[(r\,\mathrm{Re})^2 + \mathrm{B} - T]^2 + 4\mathrm{B}T},$$

$$r = \left|\frac{dp}{dx}\right| h^2/\eta_\infty u,$$

where $\left|\frac{dp}{dx}\right|$ is the magnitude of the pressure gradient in the main channel. The constant r (pressure gradient) was determined by a solution of the transcendental equation

$$\psi_0(1) = 1. \tag{10}$$

Condition (10) means that the average velocity, determined according to the distribution (8), coincides with the velocity u, chosen as the unit of measurement.

On the solid boundaries AH and BCDEFG, the stream function must be a constant, corresponding to the distribution (8):

$$\psi = 0 \text{ on } BCDEFG,\ \psi = \psi_0(2) \text{ on } AH. \tag{11}$$

The value of the vorticity $\varphi$ on the solid boundaries depends on the structure of the motion in the region and for this reason is determined during the calculation.

Equations (4)-(6) with boundary conditions (7) and (11) permit determining the stream function field and vorticity, corresponding to a stationary flow of displaced fluid.

We will study the displacement process itself assuming that the displaced and displacing fluids have the same density and viscosity. Such conditions are usually not realized in practice, but the results of experiments on models (Sec. 3) show that the behavior corresponding to the existence of two different displacement

regimes exists both when the properties of the displaced and displacing fluids are nearly the same, as well as in the case when the density and viscosity of the fluids differ considerably.

Let us assume that at some time, taken as the origin, the displacing fluid begins to flow into the inlet AB. If the displacing and displaced fluids have the same density and viscosity, then the movement of the displaced fluid into the channel does not change the structure of the flow significantly. Then, the displacement process can be studied by solving the equation for the concentration, considered against the background of the unchanged flow structure (the same as in the initial state).

Let us introduce the concentration C of the displacing fluid in the usual manner as the ratio of the mass of the displacing fluid in some volume to the total mass of this volume. The equation for the concentration assuming a constant diffusion coefficient has the form

$$\frac{\partial C}{\partial t}+\frac{\partial \psi}{\partial y}\frac{\partial C}{\partial x}-\frac{\partial \psi}{\partial x}\frac{\partial C}{\partial y}=\frac{1}{\mathrm{Pe}}\left(\frac{\partial^2 C}{\partial x^2}+\frac{\partial^2 C}{\partial y^2}\right), \tag{12}$$

where Pe = uh/D is Peclet's number (D indicates the diffusion coefficient). The quantity h/u is chosen as the time unit in Eq. (12).

The boundary conditions for Eq. (12) are as follows.

On the solid boundaries, the condition expressing the absence of a flow of matter through the boundary must be satisfied. For this reason

$$\frac{\partial C}{\partial x}=0 \text{ on } CD,\ EF,\quad \frac{\partial C}{\partial y}=0 \text{ on } BC,\ DE,\ FG,\ AH. \tag{13}$$

At the inlet, the concentration is assumed to be unchanged:

$$C=1 \text{ on } AB, \tag{14}$$

while the concentration at the outlet GH is computed.

Thus, a solution of the problem of displacement separates into two stages.

In the first stage, the structure of the stationary flow is determined. Equations (4)-(6) are solved numerically using a finite difference method. A different scheme is used approximating the first derivatives of the vorticity $\varphi$ in Eq. (4) by one-sided differences, oriented against the flow, and the remaining derivatives are approximated by central differences. In order to solve the difference equations, Libman's iteration method with successive lower relaxation is used. The values of the vorticity on the solid boundaries are calculated according to Tom's formulas [3].

The displacement process is studied directly at the second stage by numerically solving the nonstationary equations for the concentration (12). The concentration distribution for which C = 1 along the line AB and C = 0 at the rest of the points in the region is used as the initial condition. In order to solve (12) by a finite difference scheme, the line iteration scheme is used [4].

Let us consider the method for calculating the values of the concentration at points of the outlet cross section of the region GH. Let the index i, enumerating the vertical (parallel to the y axis) series of the grid, assume the value N on GH. Let us calculate $C_{N,K}$ (K is the index enumerating the horizontal rows of grid points) using a Taylor expansion near the point (N − 2, K)

$$C_{N,K}=C_{N-2,K}+\left(\frac{\partial C}{\partial x}\right)_{N-2,K}2\Delta x+\frac{1}{2}\left(\frac{\partial^2 C}{\partial x^2}\right)_{N-2,K}(2\Delta x)^2, \tag{15}$$

where Δx is a step in the grid. In order to eliminate the second derivative, entering into Eq. (15), we perform a similar expansion in the opposite direction:

$$C_{N-4,K}=C_{N-2,K}-\left(\frac{\partial C}{\partial x}\right)_{N-2,K}2\Delta x+\frac{1}{2}\left(\frac{\partial^2 C}{\partial x^2}\right)_{N-2,K}(2\Delta x)^2. \tag{16}$$

Eliminating the quantity $\left(\frac{\partial^2 C}{\partial x^2}\right)_{N-2,K}$ from Eqs. (15) and (16) and approximating $\left(\frac{\partial C}{\partial x}\right)_{N-2,K}$ by central differences, we obtain

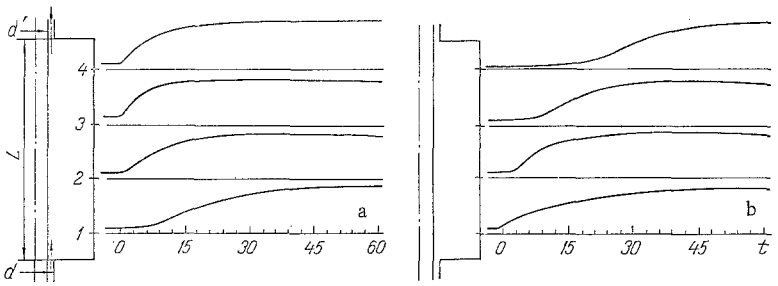


Fig. 3. Axial section of the model of a well with a cavity and graphs showing the concentration of the displacing fluid (electrical conductivity of the fluid) as a function of time t (sec) for four sections near the bottom of the cavity: a) u = 2.0 m/sec; b) 0.2 m/sec.

$$C_{N,K} = C_{N-4,K} + 2(C_{N-1,K} - C_{N-3,K}). \tag{17}$$

Calculations using Eq. (17) are performed after each whole step in time, and the newly computed values are then used on the right side of (17).

2. We will now examine some of the computational results. Analysis of the results shows that the structure of the flow and the nature of the displacement depend strongly on the ratio of Hedstrem's and Reynolds numbers. Below, we present the results concerning two (in a known sense) limiting cases of low (T = 12, Re = 1800) and high (T = 12, Re = 10) magnitudes of the ratio T/Re. Fig. 1a shows the shape of the streamlines for these two cases (the dimensions of the cavity are H = 4 and L = 8).

The difference in the flow structures also leads to a difference in the concentration distribution in the region. For high Re, the isolines of the concentration approach a direction that is parallel to the main flow, almost not penetrating into the hole, while for R = 10 the C isolines situate themselves almost transverse to the flow.

It is convenient to examine the development of the displacement process in time using diagrams constructed from the concentration fields. In these diagrams, the parts of the channel occupied mainly by the displacing fluid are shaded; examples of such regions are locations where $C > 0.65$. Fig. 2a and b shows the results of the calculations of the displacement process corresponding to Fig. 1a and b (in these calculations it was assumed that the Peclet number is Pe = 0.1 Re, and the values of the dimensionless time are indicated in the figures).

The diagrams in Fig. 2a show that for small values of the ratio T/Re the displacing fluid first fills the channel. In this situation, the cavity begins to be filled at the edge on the far side of the inlet due to the jet flowing onto the rear wall of the cavity (Fig. 1a).

For large values of T/Re, as can be seen from Fig. 2b, the channel and the cavity are filled by the displacing fluid almost simultaneously. The substitution of the content of the cavity in this case begins with the front edge of the cavity It should be noted that the diagrams in Fig. 2a correspond to much lower values of the dimensionless time than the diagrams in Fig. 2b, since the unit of measurement of time in Eq. (12) contains the pumping velocity in the denominator.

3. The existence of the different flow regimes described above is also supported by the experimental data.

The model of the well with the cavity (Fig. 3a shows the cross section of the model by a surface passing through the axis) consisted of a polyvinyl chloride plastic tube with a diameter d' = 38 mm modeling the casing and a tube with d = 50 mm with an axially symmetric cavity having a diameter of D = 160 mm modeling the well wall with a cavity. The length of the cavity L = 300 mm, the depth is H = (D-d)/2 = 55 mm, and the width of the channel is h = (d-d')/2 = 6 mm. The model was connected to a hydraulic system with a centrifugal pump. Mud with the parameters $\rho = 1.2 \cdot 10^3$ kg/m$^3$, $\eta_\infty = 1 \cdot 10^{-2}$ kg/sec·m, and $\tau_0 = 2$ N/m$^2$ was used as a displaced fluid. An aqueous solution of modified methylcellulose and calcium chloride was used as a displacing fluid.

In order to determine the degree of displacement, we used the fact that the electrical conductivity of the displacing fluid is much greater than the electrical conductivity of the displaced fluid: in this situation the

electrical conductivity of the mixture depends on the concentration of the displacing fluid. The change in the electrical conductivity near the bottom of the cavity was monitored in four sections of the cavity with the help of four pairs of measuring electrodes (in Fig. 3a, the electrodes are indicated by numbers), entering into the fluid to a distance (D-d)/6 from the bottom of the cavity. The magnitude of the current between a pair of electrodes, proportional to the electrical conductivity of the fluid, was recorded with the help of an N004M1 light beam oscillograph. Figure 3 shows the change in the electrical conductivity (concentration of the displacing fluid) with time in each of the four sections.

The initial condition in the experiment (as in the calculations of Secs. 1 and 2) consisted of a stationary flow of the displaced fluid. This state corresponds to minimum electrical conductivity of the fluid in the cavity (horizontal parts of the figure). Figure 3a and b shows the results of two experiments, differing by the fluid pumping rate (the pumping rate u was determined as the average volume velocity of motion of the fluid in the gap). The density of the displacing fluid was close to the density of the displaced fluid, the difference not exceeding 6% ($\rho = 1.22 \cdot 10^3$ kg/m$^3$ and $\rho = 1.28 \cdot 10^3$ kg/m$^3$).

For higher pumping velocities u = 2.0 m/sec (Fig. 3a) substitution of the mud by the displacing fluid at the bottom of the cavity begins at sections 3, 4 far away from the inlet (in Fig. 3 the fluid flows from bottom to top). In these sections, the electrical conductivity (concentration of the displacing fluid) increases most rapidly with time. For u = 0.2 m/sec (Fig. 3b), the concentration of the displacing fluid in the cavity begins to increase first in section 1 closest to the inlet. This property of the change in the concentration corresponds to the displacement regime obtained in the calculations in Section 2 for low values of the Reynolds number (Fig. 2b).

Thus, the results of the experiments qualitatively support the data of the numerical calculations. It should be noted that the existence of two different displacement regimes is also observed in experiments, where the densities of the displacing and displaced fluids differ by a large amount.

## NOTATION

x and y, Cartesian coordinates; h, half-width of the gap; H, L, dimensionless depth and length of the cavity; $v_x$, $v_y$, velocity components; $\rho$, density; $\tau_{ik}$, components of the viscous stress tensor; $e_{ik}$, components of the deformation rate tensor; $\eta$, dynamic viscosity; $\eta_\infty$, dynamic viscosity for infinitely high displacement velocity; $\tau_0$, analog of the limiting shear stress in Bingham's fluid; W, parameter in Williamson's model; $\nu = \eta/\eta_\infty$, dimensionless viscosity; $\psi$, stream function; $\varphi$, vorticity; $\psi_0$, $\varphi_0$, distributions of $\psi$ and $\varphi$ at the inlet; r, $a$, b, and c are auxiliary constants; C, concentration of the displacing fluid; D, diffusion coefficient; Pe, Peclet's number.

## LITERATURE CITED


1. A. Kh. Mirzadzhanzade, Improving the Cementing of Oil and Gas Wells [in Russian], Nedra, Moscow (1975).
2. S. D. Cramer and J. M. Marchello, AIChE J., 14, No. 6 (1968).
3. A. Tom and K. Éiplt, Numerical Calculations of Fields in Engineering and Physics [in Russian], Énergiya, Moscow (1964).
4. N. N. Yanenko, Method of Fractional Steps in the Solution of Multidimensional Problems in Mathematical Physics [in Russian], Nauka, Novosibirsk (1967).